ILASS 2008
Sep. 8-10, 2008, Como Lake, Italy

Paper ID ILASS08-2-16

NUMERICAL STUDY OF LIQUID SPRAY FORMATION BY INTERACTION BETWEEN A PLASMA AND A LIQUID JET

Emmanuel BODÈLE, Iskender GÖKALP

ICARE–Institut de Combustion, Aérothermique, Réactivité et Environnement, CNRS
1c, avenue de la Recherche Scientifique, 45071 Orléans cedex 2, France

ABSTRACT
In order to reduce emissions of greenhouse effect gases generated by human activities and the use of fossil resources, new sources of energy have to be developed. One of the solutions could consist in the recycling of bio-wastes produced for instance by the wood industry. For increasing the conversion rate from the original wastes to the bio-fuels several approaches have to be evaluated from the energetic point of view. One of the ways could consist in the use of high energy plasmas for the generation of synthesis gas (syngas mainly composed of CO2 and H_2) from a bio-oil obtained by a fast pyrolysis of the initial wastes. This syngas can then be converted in a *Diesel* like fuel during a Fischer-Tropsch process. The plasma phase permits to increase the syngas generation compared to more classical approaches but the energetic efficiency has still to be evaluated. The work presented in this paper consists in the numerical characterization of the interactions between the plasma and the bio-oil phases and is particularly focused on the formation of the liquid spray.

INTRODUCTION

For reducing emissions of greenhouse effect gases issued from the combustion of fossil resources since several years various approaches have been investigated which mainly consist in the use of specifically cultivated plants. These methods are accused to be responsible for the increasing of the price of vegetal productions. In order to avoid these disadvantages other approaches have to be developed and can exploit for instance vegetal wastes such as those issued from the wood industry. The overall conversion process from the initial waste to the final product requires several steps of transformation which have to be accurately evaluated as well from the energetic point of view (the process should produce more potential energy than the energy consumed for the elaboration of the final product) as from the economic standpoint (the overall process should be at least as competitive as current processes).

The process presented in this paper consists in the use of a plasma torch which permits to convert a bio-oil issued from a fast pyrolysis of the initial vegetal wastes into a synthetic gas (syngas mainly composed of CO and H_2) which can then be transformed in *Diesel* like fuel during a Fischer-Tropsch procedure [1] (fig. 1). The advantage of the plasma phase is based on its high temperature which permits to limit recombinations of the products issued from the reactions. Nevertheless, interactions between the plasma phase and the bio-oil have to be accurately investigated in order to quantify the conversion rate and the possible amount of bio-oil which can be converted. This conversion rate is directly connected with the properties of both the liquid spray generated in the system (particularly dependent on the number and the size of the droplets and their locations in the domain) and the properties of the plasma phase (nature of the gas used as plasma). Moreover, the properties (viscosity, density, surface tension…) for the liquid bio-oil can vary depending on the nature of the initial vegetal wastes and on the process used for the elaboration of the bio-oil and then can influence the properties of the liquid spray in the experiment [3].

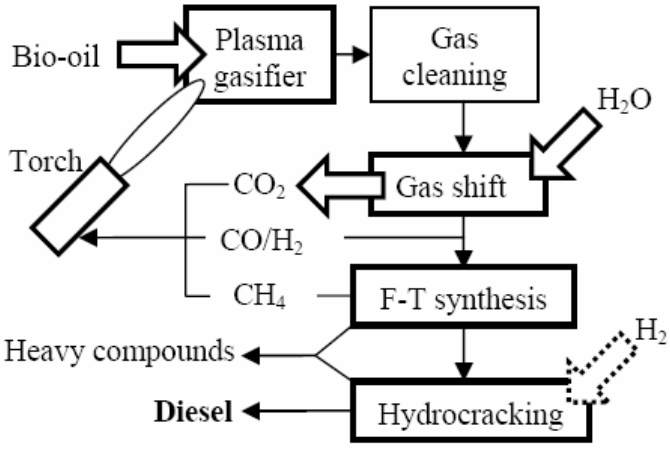

Figure 1: Schematic view of the synthetic gas and *Diesel* like fuel production process (from [2]).

This paper presents the numerical work done for the characterization of the bio-oil spray formation depending on the properties of the liquid and on the models used for the calculations. Several approaches have been tested for the treatments of interactions between the phases and especially for the models used for the characterization of the liquid fragmentation and for the behaviour of the liquid phase in the

numerical domain. Presented results mainly consist in the characterization of the liquid spray properties such as the droplet dispersion in the numerical domain and the time of residence of the droplets in the high temperature region. The influence of the fragmentation model on the final spray properties is also discussed.

NUMERICAL ASSUPTIONS

Geometry - Numerical domain

Numerical configuration reproduces as accurately as possible a reduced scale experiment dedicated to the study of a liquid bio-oil conversion by a plasma phase. This reactor is mainly composed of a 14cm in diameter cylinder in which the plasma flow generated by specific electrode is axially injected through the upper part. The resulting plasma injector diameter is equal to 15mm. The liquid is introduced in the domain through a 250µm in diameter injector located 13mm from the axis of the system and 16mm below the plasma injection plane. The total height of the domain is equal to 330mm. The detailed injection regions for both the liquid and the plasma are represented on figure 2.

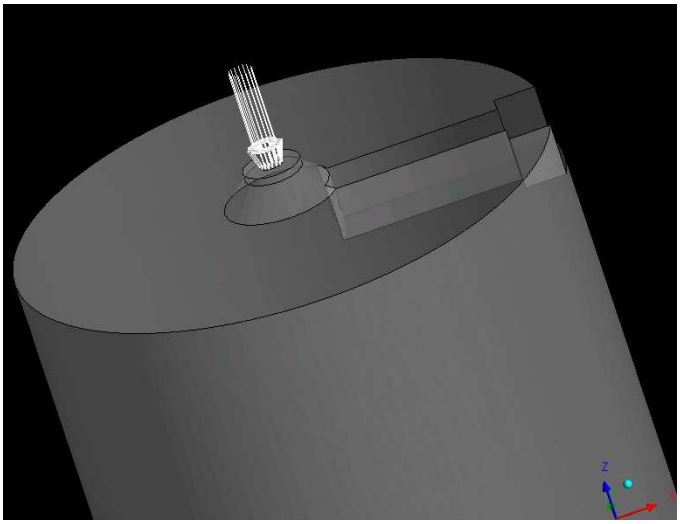

Figure 2: Detailed view of the boundary condition for the liquid and plasma injections.

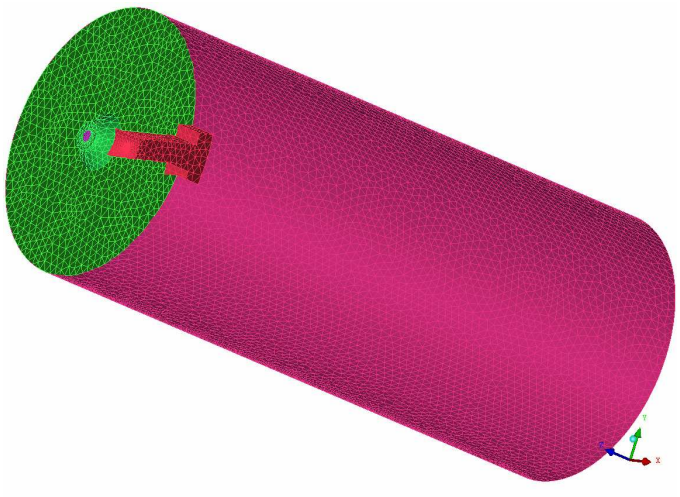

Figure 3: Global visualization of the numerical domain.

Numerical domain reproduces the global experiment using a full 3D unstructured mesh which is then composed with 631689 tetrahedrons and 110816 nodes. In order to reproduce as accurately as possible injections of both the liquid and the plasma phases and also the interaction between the phases, several refinements close to the injectors and the axis of the system have been considered. The overall numerical domain is reproduced on figure 3.

Boundary conditions

The boundary conditions consist in inlets for both the liquid and the plasma phases. The plasma is composed of argon. In order to reduce the complexity of the plasma injection (for avoiding the full calculation of the plasma ionization processes) a non ionized argon is considered instead of a real plasma. Moreover, the injection condition for this pseudo plasma phase have been modelled using a dedicated code which have permitted to obtain profiles for both the temperature and the velocity (Eqs. 1 and 2) :

$$V(r) = V_c \cdot \left(1 - (r/R)^p\right) \quad (1)$$

$$T(r) = T_c \cdot \left(1 - (r/R)^q\right) + T_a \quad (2)$$

where V_c (≈1250m/s) and T_c (≈14000K) are the centreline values for the velocity and the temperature respectively. R is the radius of the injection torch, T_a is the temperature of the anode (see ref. [2] for detailed definition of this temperature). p and q are equal to 1.2 and 2 respectively. The avaraged velocity for the plasma phase is the equal to $0.375V_c$. The plasma is introduced following the centreline of the numerical domain. The density for the plasma corresponds to the density of argon at the corresponding temperature.

The liquid bio-oil is introduced in the domain in the form of droplet with uniform diameter equal to 50µm and with a mass flow rate equal to 10g/s. The overall mass flow rate is equally introduced through 75 points uniformly distributed over the whole surface of the liquid injector. The aperture angle for the liquid injection cone is equal to 0° and the droplets are then injected perpendicularly to the surface of the injector and directly focussed in the direction of the plasma. The injection velocity for the droplet is equal to 10m/s.

The exit boundary condition consists in an "opening" condition at atmospheric pressure. This boundary is located at the lowest part of the computational domain. All other boundary conditions are walls with adiabatic condition. In order to avoid any droplet reflections and all the walls have an absorption coefficient for the liquid phase equal to 1. This condition is not supposed to play any role during calculations in reactive conditions because of the fast disappearing of the droplets in the high temperature regions of the plasma. For the plasma phase, a free slip is used on all the walls.

Liquid bio-oil thermo-physical properties

Table 1: Properties of the liquid bio-oil at T=298K

Property	Value
Density	1100kg/m^3
Viscosity	13mm^2/s
Surface tension (bio-oil in air)	37mN/m

The composition of the liquid bio-oil is very complex and contains dozens of compounds which have for the moment not been well identified. In order to perform calculations several fundamental properties such as viscosity, density or surface tension which are of major importance for the modelling of the fragmentation process have to be evaluated. A preliminary analysis of a bio-oil has given values for these properties at different temperatures [4]. These measurements have permitted to interpolate values for the temperature conditions (T=298K for the injection) used during the calculations. Corresponding values for density, viscosity and surface tension are reported in table 1.

Numerical models

In order to avoid any influence of heat and mass transfers and for an accurate characterization of the liquid fragmentation process, all the calculation have been performed using a constant thermodynamic for the liquid phase and without any heat transfers between the phases. Moreover, even if high velocities have been considered for the plasma injection the influence of the compressible effects are supposed to be negligible on the spray development process and the calculation are performed using a non compressible flow hypothesis. The liquid phase is treated using a Lagrangian approach. The momentum transfers between the phases is assured with a classic Grace law [5] because it permits at least partially to take into account deformation of the liquid droplets due to the high level of relative velocities between the phases. The turbulence for both the liquid and the plasma phases is reproduced using a classic SST (Shear Stress Transport) model [6, 7]. In order to reproduce effects of gravity on the densest phase (i.e. liquid bio-oil) the gravity has been defined in the vertical direction (the plasma is then injected following the -*z* direction).

The calculations of the liquid fragmentation process are performed with two different atomization models. First, the T.A.B. (Taylor Analogy Break-up) model [8] is used. This model permits to take into account strong deformations of liquid droplets. The resulting secondary fragments have all the same size which is adjusted in order to assume the liquid mass conservation. Second model corresponds to the Reitz & Diwakar model [9] which permits to take into account two different break-up regimes [10] and has been developed for the calculation of droplet break-up behind a shock wave. This model permits also to generate secondary droplets with various sizes.

All the calculations have been performed with the commercial CFX [6, 7] CFD code. The convergence criterion based on the root mean square of the residuals is equal to 10^{-5} for all the solved equations. The calculations are performed in two steps. The first step corresponds to the convergence of the plasma phase. After the full convergence of the calculation of the plasma phase, the liquid injection begins. This diphasic calculation is stopped after a physical time equal to 2 seconds.

NUMERICAL RESULTS

Initial plasma flow

Figure 4 presents the velocity field of the plasma phase after the convergence step. This field is obtained on a plane located at y=0 (plane located in the middle of the numerical domain which contains the domain axis and centres of both the plasma and liquid injectors). First of all, the influence of the liquid injection dedicated box plays a limited role on the behaviour of the plasma phase. Indeed, the velocity field is quasi symmetric. Moreover, plasma jet is confined in the central part of the numerical domain and then the free slip boundary condition for the plasma phase doesn't influence the behaviour of the jet. Finally, the velocity quickly decreases after the injection in the domain. The droplet will then be injected in the domain in a region where the plasma velocity is close to 600-700m/s which is lower than the maximal velocity of the plasma phase but expected to be sufficient for the appearing of liquid fragmentations. The compressible effects of the continuous phase can then be neglected which justifies the hypothesis used for the prediction of the plasma phase.

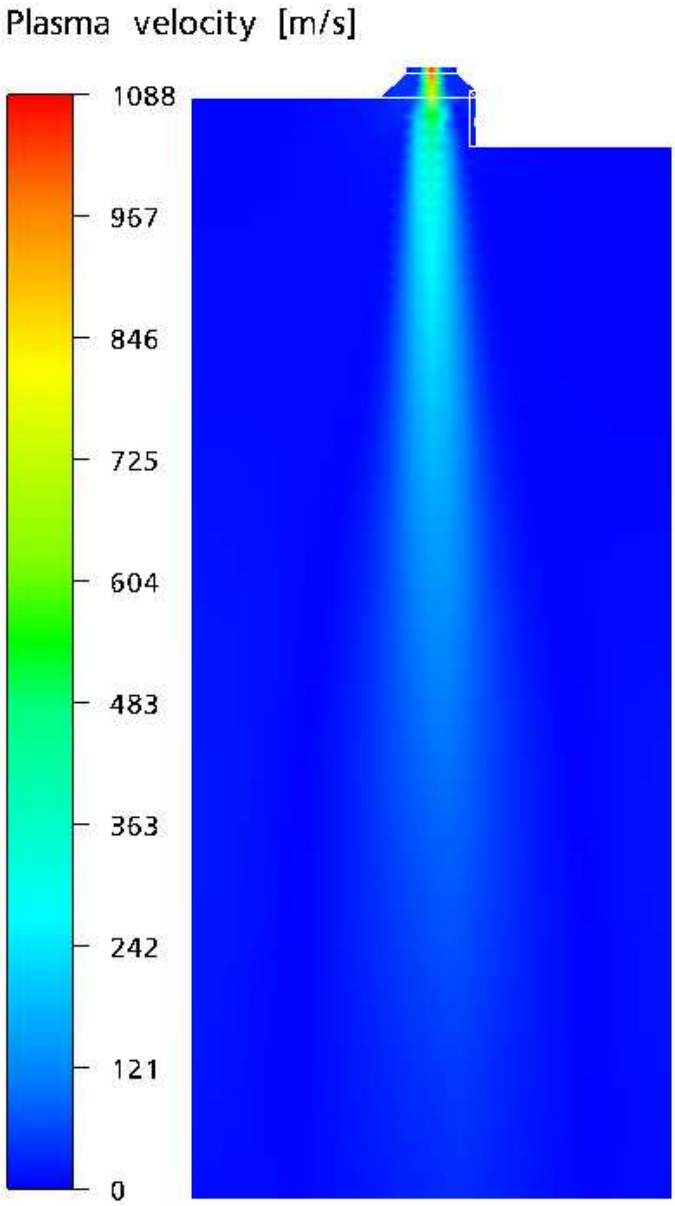

Figure 4: Visualization of the velocity field of the plasma phase after the convergence step.

Dispersion of droplets in the domain

Figure 5 presents a superimposition of the droplets in the domain with the plasma velocity field at the end of the

calculation without secondary atomization. This figure shows that the droplets exit the domain through the "opening" boundary condition at the lowest part of the domain. This is due to the constant thermodynamic hypothesis used for the calculations of the discrete phase. Indeed, droplets are supposed to be inert particles (without mass transfer, i.e. without vaporization) and can then only disappear from the domain through the walls (due to the absorption coefficient equal to 1 on the walls) or through the exit boundary condition. Moreover, droplets enter in the plasma jet region where the velocity is close to 600-700m/s and are then strongly influenced by the plasma velocity field. The influence of the gravity on the droplet trajectories is then negligible compared to the aerodynamic effects. The droplet dispersion in the domain is not significant and all the droplets remain in the central part of the domain.

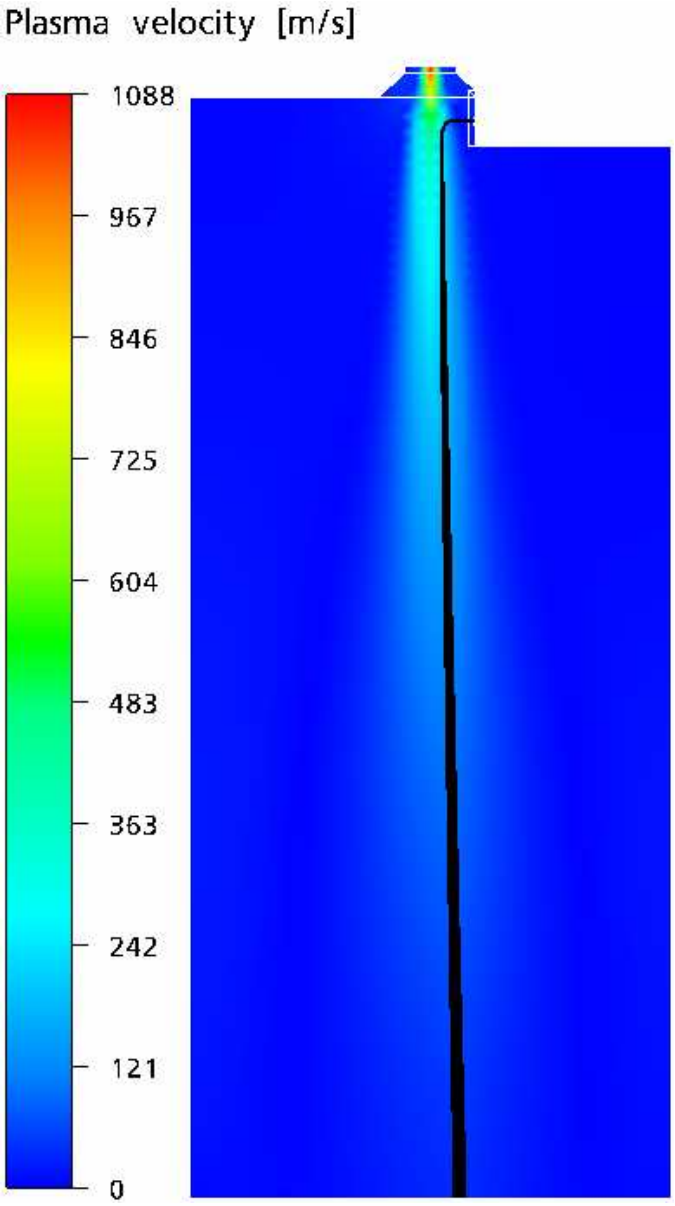

Figure 5: Superimposition of the plasma velocity field with the droplet trajectories at the end of the calculation.

Finally, the plasma jet is not influenced by the presence of the droplets. Indeed, the velocity field remains unchanged compared to the field presented on figure 4 even if a "two ways coupling" method is used for the prediction of the momentum transfers between the discrete and the continuous phases.

Very similar behaviours are observed for the two calculations with secondary fragmentation (with the T.A.B. model or the Reitz & Diwakar model) and are not represented. The influence of the atomization model is negligible on the dispersion of the droplets in the domain.

Droplet relative velocity

Figure 6 presents mean relative velocity between the continuous plasma phase and the droplets as a function of the distance from the liquid injector. This mean relative velocity is obtained by averaging the droplet velocity over the different droplet trajectories existing in the domain. On this figure, only the first 10cm have been considered because all the fragmentation processes are expected to be located in this high velocity region. This corresponds to the first upper third of the numerical domain. On this figure the results for the 3 calculations performed (i.e. without fragmentation, with T.A.B. model and with the Reitz & Diwakar model) are reported.

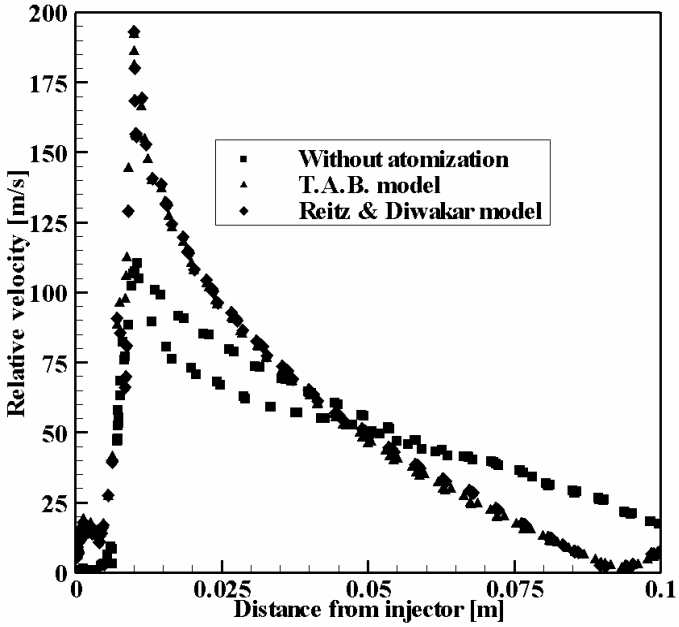

Figure 6: Mean relative velocity between the phases as a function of the distance from the injector

This figure illustrates the differences between the calculation performed without secondary fragmentation on one side and those performed with secondary atomization on the other side. Indeed, the calculation without atomization conducts to lower values for the relative velocity compared to the two other calculations. The decreasing of this relative velocity far from the injector (i.e. for distance higher than 0.025m) is less rapid in the case of the calculation without secondary atomization because of the highest inertia of these bigger droplets. Moreover, the two calculations with secondary atomization give very similar results concerning this relative velocity, even if the atomization model produces different droplets with different sizes. Nevertheless, the values observed for all the calculations are of the same order of magnitude, especially in the regions far from the injector (i.e. in the regions where the plasma phase is strongly decelerated for a distance higher than 0.05m).

Finally, the global behaviour for the relative velocity is similar for all the calculations. Indeed, after the displacement of the droplets in the low velocity plasma field they enter in the high velocity region and the relative velocity is then strongly increased. After this strong increasing the velocity is slowly decreased due to the combination of two effects. First, the plasma velocity decreases because of the expansion of the jet (see fig. 4). Second, because of the momentum transfer between the phases, the droplets are strongly accelerated by the plasma jet.

Droplet number rate

Figure 7 presents the mean droplet number rate as a function of the distance from the injector. This property is directly related to the number of physical trajectory represented by each calculated numerical Lagrangian trajectory. The calculation without secondary atomization shows a constant value because either the numerical or the physical trajectories are constant. Indeed, the number of droplet cannot change during the calculation because the particles are supposed to be inert and the fragmentation which is the most important phenomenon for the number of droplet is not activated.

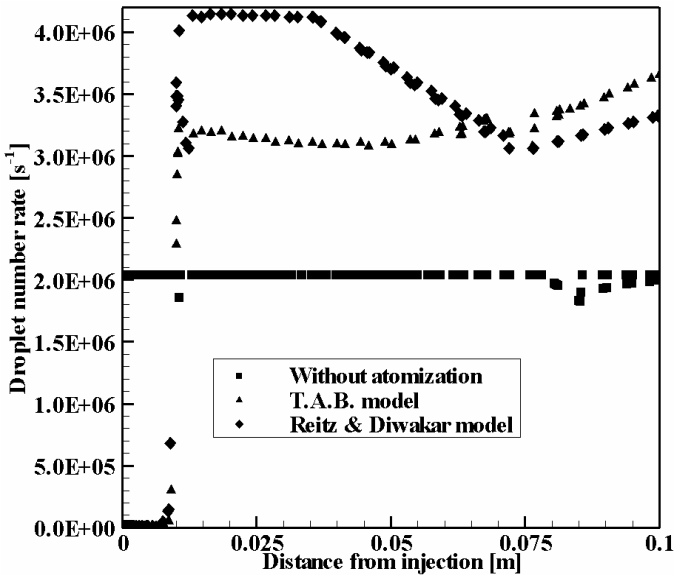

Figure 7: Droplet number rate as a function from the injector.

In the case of calculations with secondary atomization, the number rate is strongly increased compared to the calculation without atomization. This strong increasing is the consequence of the generation of smaller liquid fragments during the atomization process. Moreover, differences depending on the nature of the atomization model can be observed. In the case of the calculation with the Reitz & Diwakar model, the droplet number rate is higher than in the case of the calculation using the T.A.B. model. This behaviour is the direct consequence of the difference for the generation of secondary fragments by each model. In the case of the Reitz & Diwakar model, the number of secondary fragments is more important than in the case of the T.A.B. model. Nevertheless, both the Reitz & Diwakar and the T.A.B. models produce similar behaviour for this droplet number rate. Indeed, after the very strong increasing of the number rate due to the atomization process, the values are more or less constants when the distance from the injector is increased. This demonstrates that the most important part of the fragmentations of the droplets takes place when the droplets enter into the high velocity plasma jet and that the atomization atomization process doesn't exist anymore far from the injection.

Finally, compared to the calculation without secondary atomization, the droplet number rate is increased by about 1.6 with the T.A.B. model whereas in the case of the calculation with the Reitz & Diwakar model it is increased by about 2.

Mean diameters

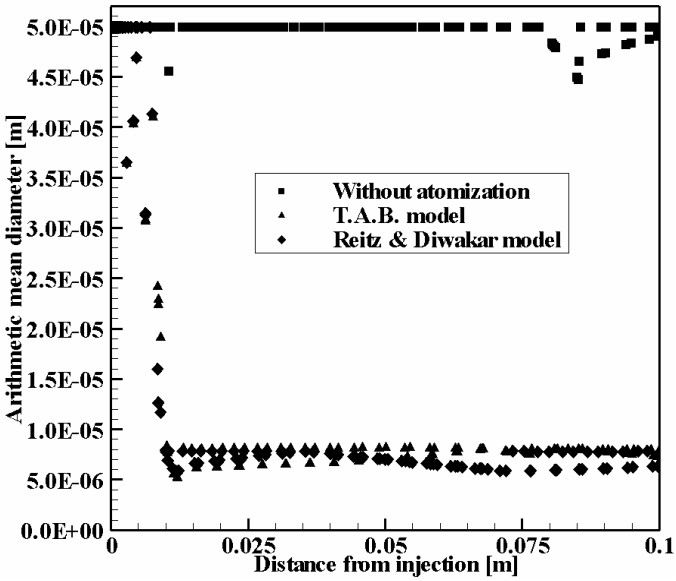

Figure 8: Arithmetic mean diameter D_{10} as a function of the distance from the injector.

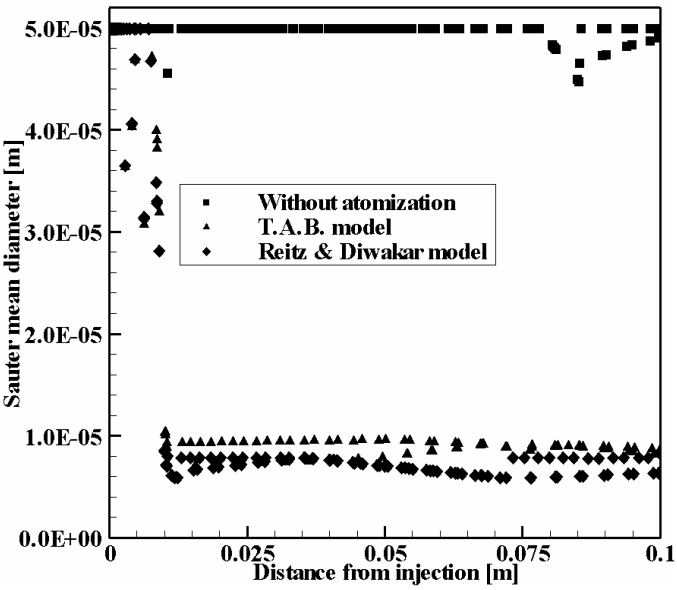

Figure 9: Sauter mean diameter D_{32} as a function of the distance from the injector.

Figures 8 and 9 present respectively evolutions of the arithmetic D_{10} and Sauter D_{32} mean diameters as a function of the distance from the injector. These figures point out the

strong influence of the atomization models on the mean diameters. Indeed, the mean diameters are divided by a factor 5 for both the arithmetic and the Sauter mean diameter. These mean diameters are then close to 10µm. Moreover, these pictures show one more time that the atomization process takes place very close to the liquid injection. Indeed, after a very strong decreasing of the mean diameters due to the penetration of the droplet in the high velocity plasma flow they remain quasi constant for the highest distances from the injection (from 0.015m to the end of the trajectories). Furthermore, the two atomization models produce same values for arithmetic mean diameter on one side and for the Sauter mean diameter on the other side. Even if the number rate (fig. 7) varies depending on the atomization model, the final mean diameters are very close.

The Sauter and arithmetic mean diameters have similar values. This behaviour is the consequence of the droplet size distribution. Indeed, even if the models can produce droplets with different size, depending on the nature of the model or on the conditions where the break-up occurs, the final droplet distribution seems to be more or less uniform or it exists a strong majority of droplets with the same diameter which is close to 10µm (which corresponds to the arithmetic mean diameter obtained with both the Sauter and the arithmetic mean diameters).

CONCLUSIONS

The work presented in this paper, relative to the numerical study of liquid spray development due to the effects of a high temperature and high velocity argon plasma have shown the extreme sensibility of the use of a secondary atomization model. Nevertheless, the nature of this model seems to have limited influence on the final spray properties such as the means diameters or the droplet dispersion in the numerical domain.

Moreover, when a secondary atomization model is used, the fragmentation process is strongly located close to the high velocity regions.

NOMENCLATURE

Symbol	Quantity	SI Unit
D_{10}	Arithmetic mean diameter	m
D_{32}	Sauter mean diameter	m
p	Exponent for the velocity injection profile	
q	Exponent for the temperature injection profile	
r	Radial location	m
R	Plasma injector radius	m
T	Temperature	K
T_a	Anode temperature	K
T_c	Temperature at the centreline	K
V	Velocity	m/s
V_c	Velocity at the centreline	m/s
x, y, z	Locations	m

REFERENCES

[1] Boissonnet G., Process development and simulation for production of Fischer-Tropsch liquids and power via biomass gasification. Oral talk presented during International Freiberg Conference on IGCC & XtL Technologies, 16-18 June 2005.

[2] Genadou D., Lorcet H., Brothier M., Gramondi P., Michou U., Onofri F., Vardelle M. and Mariaux G., Gasification of Biomass by Thermal Plasma. *7th High Temperature Air Combustion and Gasification International Symposium*, 13-16 January 2008, Phuket, Thailand.

[3] Barrata J., Modeling of biofuel droplets dispersion and evaporation. *Renewable Energy*, vol. 33, pp. 769-779, 2008.

[4] Lorcet H., Étude bibliographique des propriétés physico-chimiques des huiles de pyrolyse issues de la pyrolyse flash de la biomasse (bio-oil), *Note de support du CEA pour le projet GALACSY*, 2007.

[5] Clift R., Grace J.R. and Weber M.E., *Bubbles, drops and particles*, Academic Press, 1978.

[6] ANSYS CFX Solver Theory Guide, Release 11, 2006.

[7] ANSYS CFX Modeling Guide, Release 11, 2006.

[8] O'Rourke P.J. and Amsden A.A., The TAB method for numerical calculation of spray droplet breakup, *SAE paper n° 272089*, 1987.

[9] Reitz R.D. and Diwakar R., Effect of drop breakup on fuel spray, *SAE paper n°860469*, 1986.

[10] Shraiber A.A., Podvysotsky A.M. and Dubrovsky V.V., Deformation and breakup of drops by aerodynamic forces, *Atomization and Sprays*, vol. 6, pp. 667-692, 1996.